Organic & Biomolecular Chemistry

PAPER

An enzyme-initiated Smiles rearrangement enables the development of an assay of MshB, the GlcNAc-Ins deacetylase of mycothiol biosynthesis†

Dirk A. Lamprecht,[a] Ndivhuwo O. Muneri,[a] Hayden Eastwood,[b,c] Kevin J. Naidoo,[b,c] Erick Strauss*[a] and Anwar Jardine*[c]

MshB is the *N*-acetyl-1-D-*myo*-inosityl-2-amino-2-deoxy-D-glucopyranoside (GlcNAc-Ins) deacetylase active as one of the enzymes involved in the biosynthesis of mycothiol (MSH), a protective low molecular weight thiol present only in *Mycobacterium tuberculosis* and other actinomycetes. In this study, structural analogues of GlcNAc-Ins in which the inosityl moiety is replaced by a chromophore were synthesized and evaluated as alternate substrates of MshB, with the goal of identifying a compound that would be useful in high-throughput assays of the enzyme. In an unexpected and surprising finding one of the GlcNAc-Ins analogues is shown to undergo a Smiles rearrangement upon MshB-mediated deacetylation, uncovering a free thiol group. We demonstrate that this chemistry can be exploited for the development of the first continuous assay of MshB activity based on the detection of thiol formation by DTNB (Ellman's reagent); such an assay should be ideally suited for the identification of MshB inhibitors by means of high-throughput screens in microplates.

Introduction

The ability to counteract the effects and consequences of oxidative stress is an important adaptation that ensured the survival of organisms in an aerobic environment.[1] Moreover, many pathogenic microorganisms also maintain virulence by resisting the oxidative killing mechanisms of the human immune system's defences. Low molecular weight (LMW) thiols play a key role in these processes by acting as redox buffers, thereby helping to maintain redox homeostasis within cells.[2] In most organisms—including humans—the principle LMW thiol is glutathione. However, many Gram-positive bacteria do not contain glutathione, and evidence suggests that they instead rely on the metabolic cofactor coenzyme A (CoA) and/or the recently discovered bacillithiol (BSH) as redox buffer.[3] The actinomycetes, which include *Mycobacterium tuberculosis* (*Mtb*), the causative agent of tuberculosis, produce mycothiol (MSH) as their principal LMW thiol.[4,5] These differences, and the essential requirement

for MSH under various stress conditions, led to the identification of the biosynthesis and utilization of this novel thiol as a potential target for tuberculosis drug development.[6]

MSH is biosynthesised from UDP-GlcNAc, L-*myo*-inositol-1-phosphate (L-Ins-1-P), L-cysteine and acetyl-CoA through the sequential action of four enzymes, designated MshA, MshB, MshC and MshD (Scheme 1).[4,7] A fifth enzyme, an as yet unidentified phosphatase tentatively named MshA2, has also been implicated in the reaction.[8] Two other enzymes also play important roles in the maintenance of MSH levels: the NADPH-dependent oxidoreductase mycothiol disulfide reductase (Mtr) is responsible for the reduction of mycothiol disulfide (MSSM) formed through the oxidation of MSH,[9,10] while the mycothiol-*S*-conjugate amidase (Mca) cleaves the cysteine amide of mycothiol-*S*-conjugates formed in the MSH-dependent detoxification of alkylating agents, free radicals and xenobiotics. In the process it forms 1-D-*myo*-inosityl-2-amino-2-deoxy-D-glucopyranoside (GlcN-Ins) and a mercapturic acid derivative, which is excreted.[11]
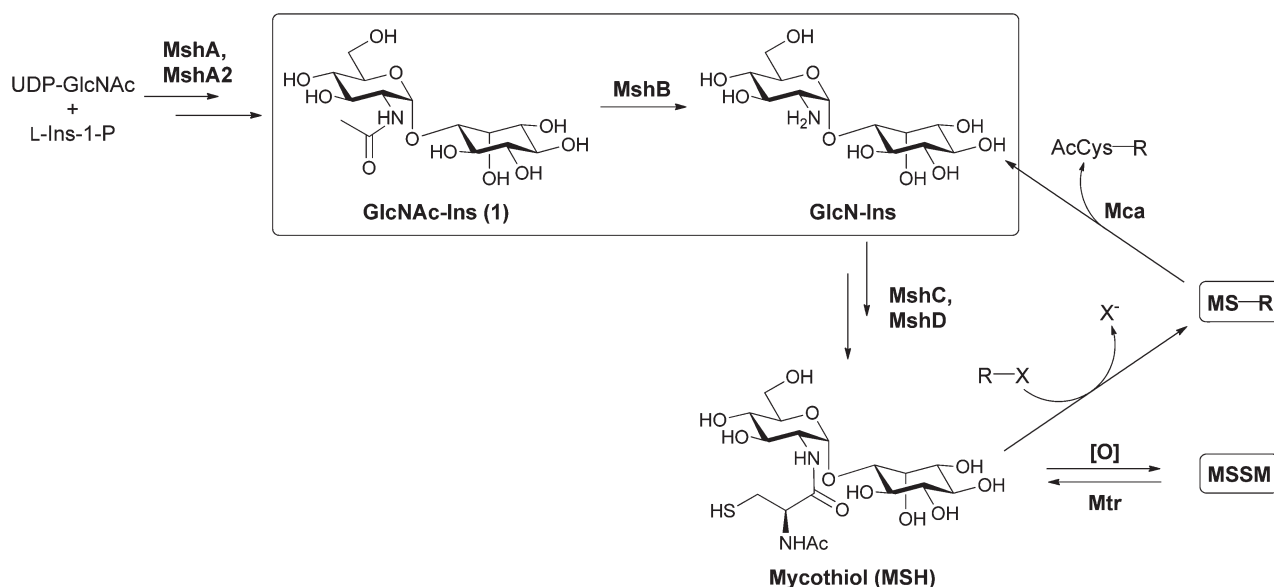
The mycothiol biosynthetic enzyme MshB is one of the enzymes in the pathway that has been identified as an attractive potential target for drug discovery. This was based on the fact that MSH levels in knockout mutants of the mycobacterium *M. smegmatis* that lacked the *mshB* gene were reduced up to 95% compared to wild-type (the low residual formation of MSH was ascribed to the promiscuous nature of Mca).[12] MshB is a metal-dependent hydrolase[13] that catalyses the deacetylation of *N*-acetyl-1-D-*myo*-inosityl-2-amino-2-deoxy-D-glucopyranoside (GlcNAc-Ins, **1**) to form the amino sugar GlcN-Ins. Structural

[a]Department of Biochemistry, Stellenbosch University, Private Bag X1, Matieland 7602, South Africa. E-mail: estrauss@sun.ac.za; Fax: +2721 808 5863; Tel: +27 21 808 5866
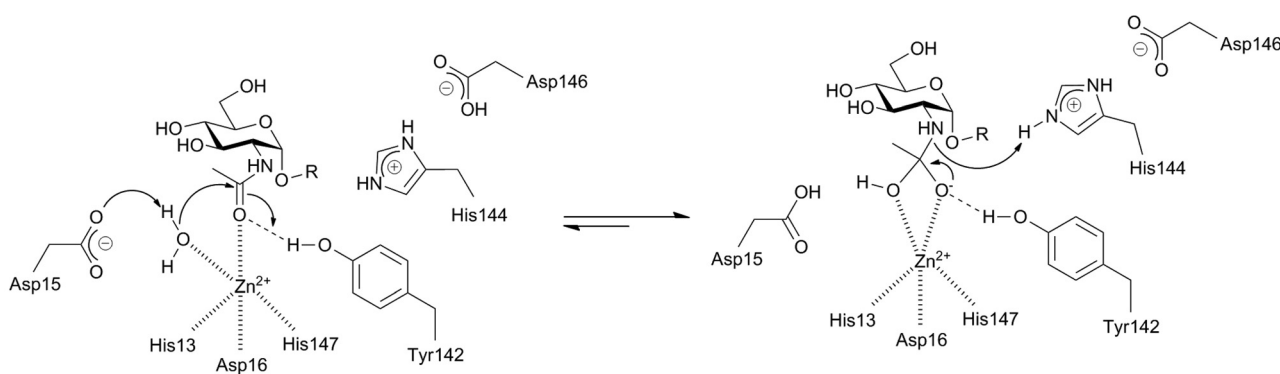*[b]Scientific Computing Research Unit, University of Cape Town, Private Bag X3, Rondebosch 7701, South Africa*
[c]Department of Chemistry, University of Cape Town, Private Bag X3, Rondebosch 7701, South Africa. E-mail: anwar.jardine@uct.ac.za; Fax: +2721 650 4010; Tel: +27 21 650 4010

5278 | *Org. Biomol. Chem.*, 2012, **10**, 5278–5288

This journal is © The Royal Society of Chemistry 2012

Scheme 1 Biosynthesis and recycling of mycothiol (MSH).

Scheme 2 Proposed catalytic mechanism of MshB, highlighting the active site residues involved in catalysis.[17]

analysis showed that the active site metal—previously thought to be zinc, although recent studies have found higher activity with iron[14]—is coordinated to two histidine residues (His13 and His147) and an aspartate (Asp16).[15,16] The metal is also bound to the acetamidocarbonyl oxygen of the substrate and a water molecule, which was proposed to be activated for nucleophilic attack through this interaction. This has been confirmed in recent mechanistic studies, which also showed that MshB uses a general acid–base mechanism in which Asp15 and His144 act as the general base and acid catalysts respectively, while Tyr142 plays a dynamic role that includes stabilization of the oxyanion intermediate (Scheme 2).[17]

The study of MshB activity and inhibition poses two major practical challenges. First, its natural substrate can only be obtained by means of lengthy multi-step synthetic procedures,[18,19] or by isolation of mycothiol-*S*-conjugates from natural sources, followed by treatment with Mca to release GlcN-Ins (Scheme 1).[20] Consequently, many recent MshB studies made use of commercially available GlcNAc (**2**) as an alternate minimal substrate instead,[14,17,21] even though it has been shown that MshB is ~100-fold less active towards this compound.[4,20] Additionally, other groups have invested

significant synthetic effort in the discovery of alternate MshB substrates that give reasonable levels of activity.[22] Second, the general method for the assay of MshB activity involves derivatization of reaction products followed by lengthy HPLC analysis, which precludes high-throughput screening.[22–24] A significant advancement has been the recent development of a fluorescence-based microplate assay that measures MshB activity based on the reaction of fluorescamine (FSA) with the free amine of the deacetylation product after the reaction has been quenched.[21] However, its mechanism precludes its use for the screening of compound libraries for potential MshB inhibitors in which similarly reactive functional groups are represented.

In this study we sought to address these shortcomings by the incorporation of chromogenic functional groups into the structures of potential alternate MshB substrates. Our strategy was to exploit any changes that occur in the absorbance spectra of such compounds upon deacetylation for use in a continuous spectrophotometric assay. In the process we uncovered an unexpected enzyme-initiated Smiles rearrangement of one of the substrates, which allowed the development of a new, sensitive microplate-based assay of MshB activity.
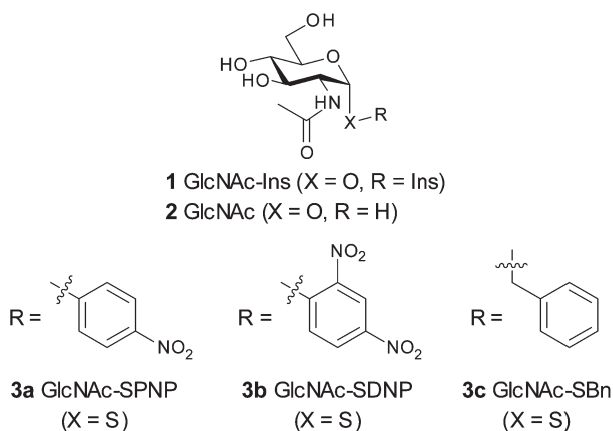
This journal is © The Royal Society of Chemistry 2012

Org. Biomol. Chem., 2012, **10**, 5278–5288 | 5279

1 GlcNAc-Ins (X = O, R = Ins)
2 GlcNAc (X = O, R = H)

R = [3a structure]   R = [3b structure]   R = [3c structure]

3a GlcNAc-SPNP   **3b** GlcNAc-SDNP   **3c** GlcNAc-SBn
(X = S)   (X = S)   (X = S)

Fig. 1 Structures of alternate MshB substrates used in this study.

Results and discussion

Rationale and strategy

Previous studies of MshB and Mca have shown that modification of the inosityl moiety of GlcNAc-Ins is usually tolerated by these enzymes, although often to the detriment of the observed activity.[19,22] We therefore chose to investigate whether the replacement of the inosityl group by aromatic moieties would similarly result in compounds accepted as substrates by MshB. More specifically, we set out to use aromatic groups that are known strong chromophores, anticipating that deacetylation of such alternate substrates may result in changes in their absorbance maxima. Such changes would allow the continuous spectrophotometric assaying of MshB activity, which would be ideal for high-throughput screening. We decided to introduce such groups *via* S-glycoside linkages, since the syntheses of several α-GlcNAc thioconjugates have been reported.[19,22,24–26]

Three aromatic groups were chosen as replacements of the inosityl group of GlcNAc-Ins for this study (Fig. 1). In the first case a *para*-nitrophenyl group, a well-known chromophore utilized in several different enzymatic assays, was selected to give GlcNAc-SPNP (**3a**). Second, a 2,4-dinitrophenyl group was chosen to give GlcNAc-SDNP (**3b**) as a potential alternate substrate. The extra nitro-group was expected to increase the absorbance intensity of the chromophore, thereby potentially also increasing its sensitivity to any changes that might occur in its absorbance spectrum upon deacetylation. Third, a simple benzyl group was selected as a reference for the study of the other two groups, as its absorbance was unlikely to be affected by deacetylation due to its distant location from the acetamido group. Moreover, a recent study found that GlcNAc-SPh (the phenyl thioglycoside) showed ~30% of the activity of the native GlcNAc-Ins substrate, suggesting that GlcNAc-SBn (**3c**) might similarly act as a good alternate substrate, thereby also acting as a positive control.[22]

Docking studies and computational chemistry

One of the alternate substrates that we proposed to use in this study, the dinitrophenyl derivative **3b**, was recently reported to be inactive in a MshB assay that depended on the fluorescent
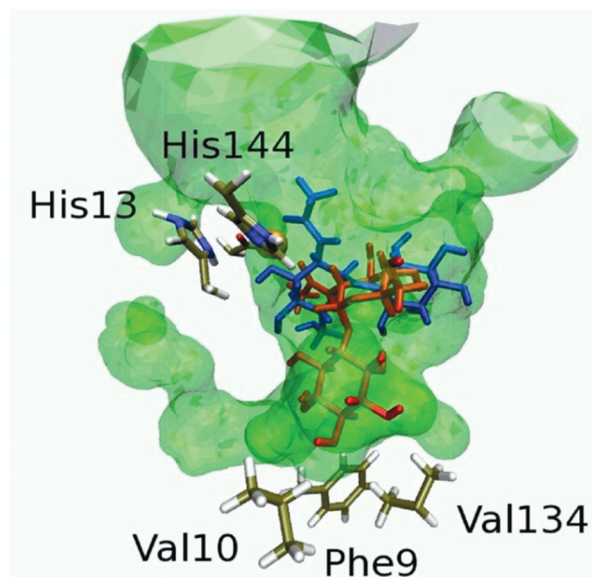

Fig. 2 Molecular docking analysis of the MshB active site binding pocket (enclosure shown in green) identifies two possible binding orientations for the native substrate GlcNAc-Ins (**1**), shown in red (geometry 1) and blue (geometry 2) respectively. His13 which coordinates zinc, and the general acid catalyst His144 are shown, as well as the hydrophobic residues at the base of the pocket.

derivatization of the free amine of the expected product, followed by HPLC analysis.[22] While this result indicated that **3b** would not be suitable for the purposes of this study, it seemed curious in light of the good activity observed for the structurally analogous GlcNAc-SPh using the same assay. Evaluation of the available structures of recombinant MshB indicated that its binding pocket is cavernous and that it should be able to accommodate a variety of substrates, as indicated by the green enclosure shown in Fig. 2.[15,16] However, charged or polar amino acids predominate in the binding cavity, with few well-defined hydrophobic regions. This suggested that the hydrophobic aromatic groups of the alternate substrates would not be accommodated in the MshB active site, although this could be offset by the potential of the nitro substituents to act as hydrogen bond acceptors. To establish whether **3a** and/or **3b** would be excluded from MshB's active site based on such structural considerations, we set out to perform docking and molecular dynamics studies using one of the available MshB structures (PDB: 1Q74).[16] While the active site zinc ion is clearly visible in this structure, it does not contain any other bound ligands. The natural substrate GlcNAc-Ins (**1**) and minimal substrate GlcNAc (**2**) were therefore also included in the analysis for comparative purposes.

The results of the molecular dynamics studies performed with the solution-equilibrated MshB structure indicated that the docked MshB–ligand complexes with good scores have the acetamidocarbonyl oxygen in close proximity to the zinc, which is consistent with the current mechanistic understanding of metal-dependent deacetylases.[13] Moreover, the relatively large active site cavity volume permits two favourable docked-ligand geometries for each of the ligands, both of which have the acetamidocarbonyl oxygen placed in a manner allowing catalysis to take place. For the natural substrate GlcNAc-Ins, the two binding
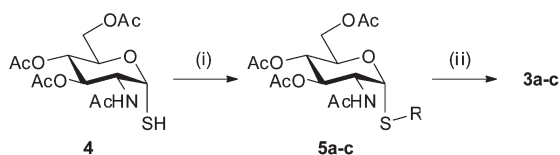
Scheme 3 Synthesis of thioglycosides **3a–c**. (i) 1-fluoro-4-nitrobenzene (for **a**), 1-fluoro-2,4-dinitrobenzene (for **b**) or benzyl bromide (for **c**), Et₃N, CH₂Cl₂, 25 °C. (ii) MeOH, H₂O, acetone, Amberlite IRA-400 (OH⁻). The R-groups are defined in Fig. 1.

pocket orientations can be defined using its coordination to the zinc ion as pivot, and its displacement relative to His13 and Asp16 as reference points (Fig. 2). In geometry 1, GlcNAc-Ins extends into a pocket facing down and away from His13, while in geometry 2 GlcNAc-Ins stretches across into a binding pocket that is orthogonal to geometry 1. The results indicate that for GlcNAc-Ins there may be a small but significant energetic preference for geometry 1 over geometry 2.

In regards to the alternate substrates, the docking analysis indicates that the minimal substrate GlcNAc (**2**) prefers binding in geometry 2, which may partially explain its reduced activity. Similarly GlcNAc-SPNP (**3a**) also prefers binding in geometry 2, while GlcNAc-SDNP (**3b**) prefers geometry 1. The analysis also shows that regardless of the binding geometry, the aromatic rings of both proposed alternate substrates can be accommodated in the same pocket that binds inositol. However, the presence of the hydrophobic residues Val10, Phe9 and Val134 at the base of the pocket that surrounds geometry 1 would seem to indicate that this would be the binding mode most likely to compensate for the loss of the various hydrogen bonding interactions when the inosityl moiety of GlcNAc-Ins in replaced by an aromatic group.

Taken together, the results of the docking studies suggest that **3a** and **3b** would most likely act as alternate substrates for MshB, with activities similar to that previously observed for GlcNAc-SPh.[22]

Synthesis of potential chromogenic substrates of MshB

The α-GlcNAc-mercaptan (**4**) has previously been used in the synthesis of a range of α-thioglycosides—including analogues of MSH—by simple nucleophilic substitution using an appropriate electrophile.[19,26] We therefore decided to expand on this established chemistry for the synthesis of the α-thioglycosides **3a–c** (Scheme 3). Triethylamine-mediated *S*-alkylation of **4** with aryl fluorides or benzyl bromide gave the desired *O*-acetylated thioglycosides (**5a–c**). Subsequent *O*-deacetylation gave the unprotected thioglycosides (**3a–c**). As expected, the coupling constants of the anomeric protons were all consistent with that of α-coupled thioglycosides.

Confirming MshB activity with alternate substrates by HPLC

With the thioglycosides **3a–c** in hand we set out to demonstrate that these are indeed accepted by MshB as alternate substrates. The UV-visible spectra of **3a–c** showed that, as predicted, the nitrophenyl-containing **3a** and **3b** have large extinction
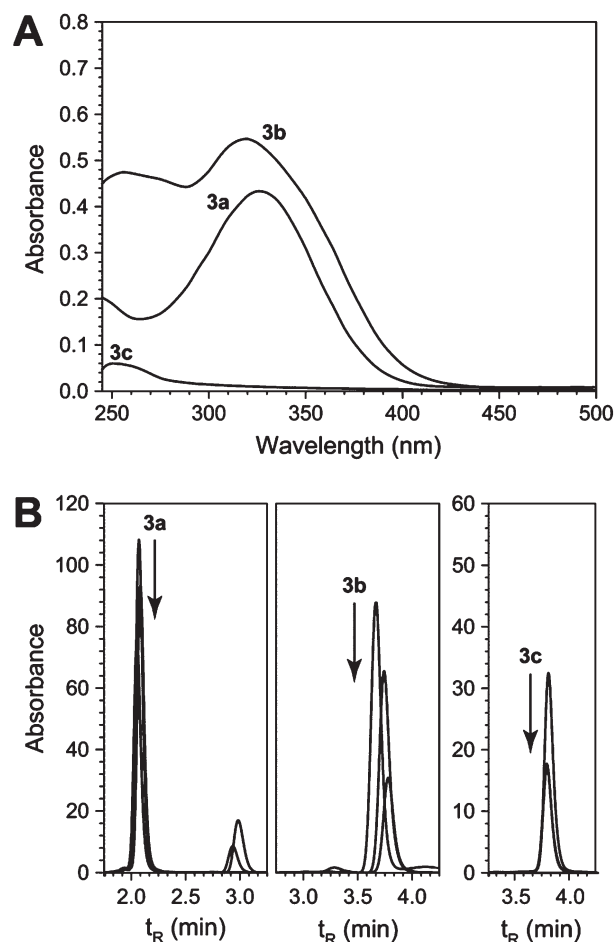
Fig. 3 Characterization of **3a–c** as potential alternate MshB substrates. Panel A, UV-vis spectra of **3a–c** at 200 μM. Panel B, HPLC analysis of 100 μM each of **3a**, **3b** (at 320 nm) and **3c** (at 254 nm) incubated in the presence of MshB followed by heat inactivation at set time intervals, shows a time-dependent decrease in the concentration of each compound.

coefficients at ∼325 nm and ∼320 nm respectively, while the benzyl-containing **3c** has a relatively poor absorbance with a maximum at ∼254 nm (Fig. 3A). Nonetheless, the presence of the chromophoric groups in all three cases allowed their direct analysis by HPLC, which provided for a simple method whereby their potential deacetylation by MshB could be monitored. Subsequent incubation of MshB individually with 100 μM each of **3a–c** showed a time-dependent decrease for all three compounds, confirming that they indeed act as alternate substrates of the enzyme (Fig. 3B). Integration of the peak area at each time point allowed for the HPLC results to be converted to time-course data by comparison to a standard curve prepared independently. In this manner the specific activity of the enzyme towards each substrate could be calculated (Table 1). These values indicated that MshB has a similar specific activity for all three the alternate substrates, which is ∼12% of the value previously determined for the natural substrate GlcNAc-Ins using HPLC analysis of the fluorescent derivative of the product.[27] However, it is about an order of magnitude better than the value determined for the minimal substrate GlcNAc in the same manner, indicating that

Table 1 MshB activity of various substrates as measured by using the indicated assays[a]

Assay	Substrate	Specific activity (nmol min^{-1} mg^{-1})	Rate (V/E)[b] (min^{-1})
HPLC (AccQ-Fluor deriv.)[c]	GlcNAc-Ins (**1**)	220 ± 40[27]	7.21 ± 1.31[27]
	GlcNAc (**2**)	3 ± 2[27]	0.10 ± 0.07[27]
HPLC (direct)[d]	GlcNAc-SPNP (**3a**)	26.9 ± 1.3	0.88 ± 0.04
	GlcNAc-SDNP (**3b**)	28.4 ± 3.0	0.93 ± 0.10
	GlcNAc-SBn (**3c**)	25.4 ± 3.0	0.83 ± 0.10
Fluorescamine (FSA)[e]	GlcNAc (**2**)	19.1 ± 3.4	0.63 ± 0.11
	GlcNAc-SPNP (**3a**)	∼0	∼0
	GlcNAc-SDNP (**3b**)	4.2 ± 3.7[f]	0.14 ± 0.12
	GlcNAc-SBn (**3c**)	122.2 ± 17.0[f]	4.01 ± 0.56
DTNB[e]	GlcNAc (**2**)	∼0	∼0
	GlcNAc-SPNP (**3a**)	∼0	∼0
	GlcNAc-SDNP (**3b**)	145.8 ± 15.9	4.78 ± 0.52
	GlcNAc-SBn (**3c**)	∼0	∼0

[a] Activity values determined in this study represent the average of three independent measurements, with the standard error shown. [b] Calculated from the specific activity data. [c] Using 100 μM substrate in water, and 0.5 μM MshB. [d] Using 100 μM substrate in water, and 2 μM MshB. [e] Using 5 mM substrate in 5–10% DMSO, and 1 μM MshB. [f] Based on a standard curve prepared with GlcN.

the thioglycosides **3a–c** may act as suitable alternative substrates for the assay of MshB activity.

Confirmation of the formation of the expected products upon deacetylation of 3a–c by MshB

Since synthetic standards of the expected deacetylation products of **3a–c** were not available, the HPLC-based MshB activity assay described above could only be used to confirm the disappearance of substrate and not the formation of these products. To confirm that MshB treatment of **3a–c** yields products containing free amino groups, we employed the recently reported MshB assay in which its substrate (GlcNAc in the original description) is incubated in the presence of the reactive fluorophore FSA.[21] The FSA reacts with the free amine of the deacetylated product as it is formed to give a fluorescent conjugate, thereby providing for the monitoring of product formation—and consequently MshB activity—by fluorimetry.

The activity of MshB towards GlcNAc and the thioglycosides **3a–c** (5 mM in 10% DMSO) were monitored in this manner over a period of 1 h. The observed increase in fluorescence for each substrate over time was subsequently converted to a change in concentration over time using a standard curve prepared from known concentrations of glucosamine (GlcN); in doing so, the assumption was made that the reactivity of the deacetylated products of **3a–c** towards fluorescamine would be similar to GlcN, and that the rates obtained in this manner (after adjustment for any background using a control sample containing no substrate)

would allow for a direct comparison of the activity of MshB towards the respective substrates.

Surprisingly, the resulting data (Table 1) gave rise to a very different activity profile than the one determined by HPLC analysis. The FSA-based assay highlights GlcNAc-SBn **3c** as being the preferred MshB substrate among the thioglycoside, showing a specific activity ∼6-fold that of GlcNAc **2**, while GlcNAc-SPNP **3a** and GlcNAc-SDNP **3b** show no or very low activities (with large errors). Since the HPLC-based assay clearly indicated the disappearance of all three thioglycosides, this finding suggested that the products formed upon deacetylation of **3a** and **3b** do not contain free amine groups that are available for reaction with FSA. We next set out to establish a possible mechanistic basis for such an outcome.
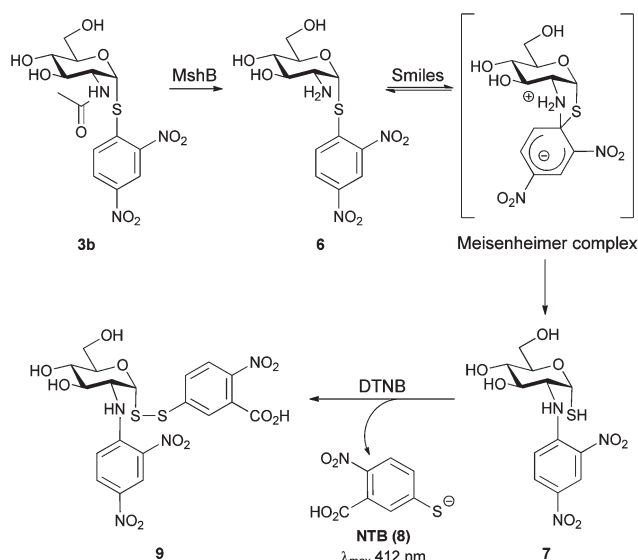
Deacetylation of GlcNAc-SDNP unmasks a free thiol: an enzyme-initiated Smiles rearrangement

We considered that the unmasking of the free amino group of **3a** and **3b** could lead to a possible intramolecular rearrangement that results in this group being blocked again, thereby preventing their reaction with FSA. Such a case was reported by Kondo *et al.*, which found that *S*-(2,4-dinitrophenyl)cysteine undergoes a facile base-catalyzed S → N rearrangement to form *N*-(2,4-dinitrophenyl) cysteine.[28] This type of rearrangement, which falls under a broad category of intramolecular aromatic nucleophilic substitution reactions, involves the formation of an anionic σ complex intermediate, also referred to as a Meisenheimer complex. Such rearrangements were first reported by Smiles in 1930, and are therefore known by his name.[29] In the experiment by Kondo *et al.*, the reaction was performed by incubating *S*-(2,4-dinitrophenyl)cysteine with different organic bases, including imidazole. This suggested that enzyme-borne bases could also promote such Smiles rearrangements, and that this could be the basis for the surprise finding that **3a** and **3b** are seemingly inactive in the FSA-based MshB assay.

A Smiles rearrangement of the thioglycoside substrates after deacetylation by MshB should unmask a free thiol group, as shown for **3b** in Scheme 4. Since the concentration of free thiols can be established through reaction with 5,5′-dithiobis-(2-nitrobenzoic acid) (DTNB, or Ellman's reagent), GlcNAc (acting as negative control) and **3a–c** was individually incubated with MshB. The reactions were stopped at set time intervals, followed by treatment with DTNB and measurement of the increase in absorption at 412 nm to determine the rate of formation of 2-nitro-5-thiobenzoate (NTB, **8**), if any.

The results (Table 1) showed an increase only in the case of GlcNAc-SDNP **3b**, with none of the other substrates showing an increase above the background rate (no substrate control). Moreover, the rate observed for **3b** in this assay is very similar to the rate seen for **3c** in the FSA-based assay. This finding confirms that GlcNAc-SDNP **3b** does act as an alternate substrate for MshB, and that its apparent inactivity (based on the results of the FSA-based assay and as reported in a previous study that used AccQ-Fluor derivatization followed by HPLC analysis) is due to an S → N Smiles rearrangement.

The observation that GlcNAc-SPNP **3a** does not show a similar unmasking of its thiol, while also being unreactive in the
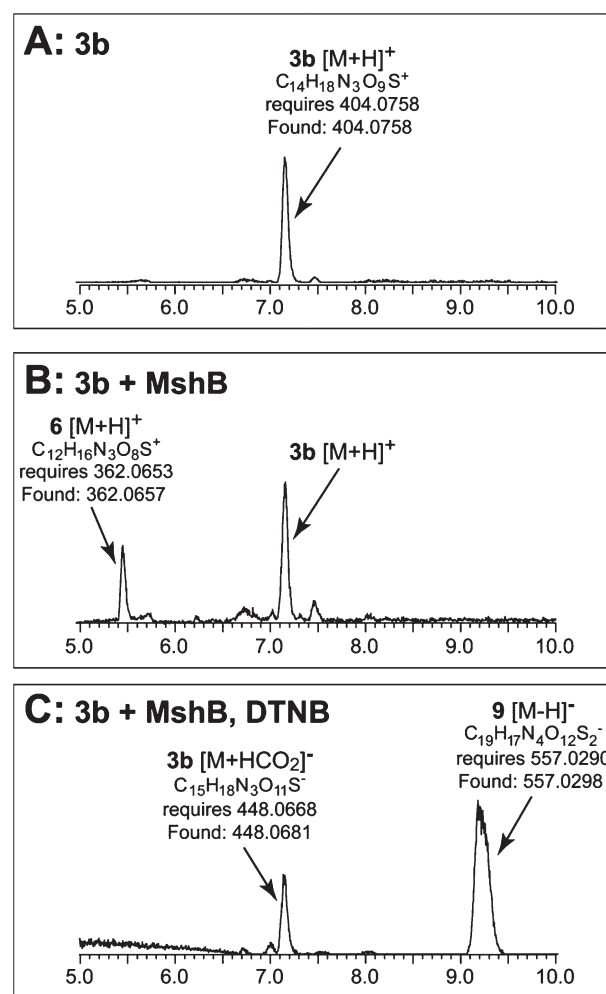
5282 | *Org. Biomol. Chem.*, 2012, **10**, 5278–5288

This journal is © The Royal Society of Chemistry 2012

Scheme 4 Proposed Smiles rearrangement of the MshB-catalysed de-acetylation product (**6**) of GlcNAc-SDNP **3b**. The formation of the rearrangement product **7** can be followed by derivatisation with DTNB (Ellman's reagent) to form the strong chromophore, 2-nitro-5-thiobenzoate (NTB, **8**) and the mixed disulfide **9**.

Fig. 4 LC-HR-ESI-MS analyses of the product(s) formed in the MshB-mediated reaction of GlcNAc-SDNP **3b**. Panel A, base peak ion (BPI) chromatogram of a control reaction mixture containing only the substrate **3b** in the presence of the reductant TCEP. Panel B, BPI chromatogram of a reaction mixture containing **3b**, MshB and TCEP. Panel C, BPI chromatogram of a reaction mixture containing **3b** and MshB (but no TCEP) that had been treated with DTNB prior to analysis. All peaks were identified by analysis of the associated mass spectra (the required and found mass for the major ion in each spectrum is shown) and observed fragmentation patterns. The full chromatograms and the associated mass spectra are provided as ESI.†

FSA assay, may be due to the reversible formation of the corresponding Meisenheimer complex that is less stabilized by the single nitro group, and which therefore does not complete the rearrangement. Since the docking studies indicated that **3a** and **3b** may prefer to take on different binding modes, this might also play a role in differentiating their activity profiles. However, no direct evidence in support of either analysis can be provided at this stage.

Identification of the Smiles rearrangement product

We subsequently set out to positively identify and study the Smiles rearrangement product by its chemical synthesis; however, all attempts in this regard failed, as all the conditions used for *N*- and/or *O*-deacetylation led to the formation of *N*-(2,4-dinitrophenyl) glucosamine and H₂S. We therefore attempted its identification by LC-HR-ESI-MS analysis instead. Comparison of reaction mixtures that contained **3b** in either the absence or presence of MshB indicated the enzyme-mediated formation of the deacetylation product **6** but not its rearrangement product **7** (Fig. 4). This identification is based on the analysis of the associated mass spectrum, which showed the formation of fragments that is in agreement with the structure of **6** but not **7**, although it is also possible that a stabilized Meisenheimer complex would give the same observed fragmentation pattern (see ESI†); note that all three structures (**6**, **7**, and the complex) have the same molecular mass. Addition of the reductant tris-(2-carboxyethyl)phosphine (TCEP) to the reaction mixtures gave the same result. To establish whether the rearrangement product is formed, but decomposes prior to or during analysis, DTNB was added to mixtures after they had been quenched and the precipitated protein removed. Samples that had been treated in this

manner, and that did not contain TCEP, showed the formation of a new peak that was identified as the mixed disulfide **9** (Fig. 4); in the presence of TCEP this peak was not observed.

The results of the LC-HR-ESI-MS analyses confirm the deacetylation of GlcNAc-SDNP **3b** by MshB to form the deacetylation product **6**, as well as its subsequent rearrangement to form **7**. Since the FSA-based assay failed to trap any free amine-containing products, it is most likely that the observation of **6** in these analyses is due to its formation from the stabilized Meisenheimer complex under the acidic conditions used for the MS analysis; the Meisenheimer complex could also give the same fragmentation pattern directly (Fig. 4B). Formation of the labile rearranged product **7** is confirmed by its trapping by DTNB to

This journal is © The Royal Society of Chemistry 2012

*Org. Biomol. Chem.*, 2012, **10**, 5278–5288 | **5283**

form the stable disulfide adduct **9**; however, in the absence of a trapping reagent **7** is not observed, in agreement with the difficulties encountered with its chemical synthesis.

Exploiting the Smiles rearrangement to develop a new MshB assay amenable to high-throughput screening

The confirmed deacetylation of GlcNAc-SDNP **3b** by MshB led us to consider whether this substrate could be used for the development of a new assay for MshB activity, which is also amenable to high-throughput screening. Towards this end, we first determined whether product formation could be measured based on changes that occur in the absorbance spectrum of **3b** upon its deacetylation (and/or subsequent Smiles rearrangement). However, incubation of **3b** in the presence of MshB showed no significant time-dependent changes in its absorbance at 320 nm (its absorbance maximum, see Fig. 3A), making direct spectrophotometric-based activity analysis impossible and necessitating an alternative strategy.

The reaction of DTNB with free thiols have been used to assay the activity of several enzymes (including the mycothiol disulfide reductase, Mtr[9]) in continuous fashion. Having confirmed the reaction of DTNB with **7** and the formation of the mixed disulfide **9** and the associated NTB (**8**) by-product, we therefore set out to determine if MshB activity could also be determined in this manner. Increasing concentrations of **3b** (between 0 and 5 mM) were incubated in the presence of MshB and DTNB, and the increase in absorbance at 412 nm monitored in a time-dependent fashion. For comparison, identical reaction mixtures were incubated without DTNB, stopped at regular time intervals, and the amount of product formed determined by DTNB treatment after the enzyme was precipitated and removed as before.

The progress curves obtained from the continuous monitoring of MshB activity through NTB release showed an initial lag period (presumably due to the slow collapse of the Meisenheimer complex) before giving way to the linear increase in NTB formation. Importantly, a control reaction that contained 100 μM substrate but no enzyme showed no increase, confirming that the observed increase in absorbance was due to enzyme activity. Regression analysis of the linear portions of the progress curves allowed for the corresponding activity rates to be calculated, while the rates from the discontinuous assay were determined from regression analysis of the data obtained at the set time-intervals at each concentration. The results (Fig. 5) show that the data obtained by either method give comparable rates at substrate concentrations of 1 and 5 mM. However, the continuous monitoring of activity is clearly superior since it gave data points with smaller errors, leading to an excellent linear correlation between activity and substrate concentration over the whole concentration range measured. In fact, when the activity of reaction mixtures with less than 1 mM substrate was determined in a discontinuous fashion, the variation in the replicates became so large that accurate measurements became impossible (data not shown). The activity obtained using 5 mM **3b** (3.4 ± 0.1 min^{-1} from the continuous assay, and 5.0 ± 1.0 min^{-1} for the discontinuous assay) also correlate well with those obtained for 5 mM GlcNAc–SBn **3c** obtained in the FSA-based assay (Table 1). This suggests that
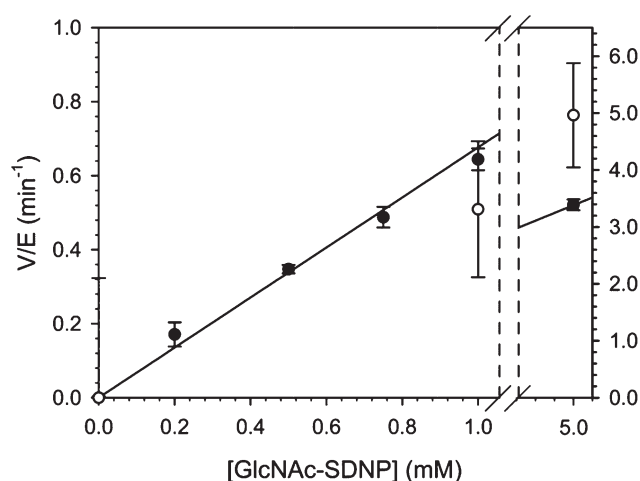
Fig. 5 Activity profile of MshB with GlcNAc-SDNP **3b** as substrate, measured based on the release of NTB (**8**) after reaction of DTNB (Ellman's reagent) with the rearranged deacetylation product **7** (see Scheme 4). Closed circles (●) represent data points determined through the continuous monitoring of product formation by performing the reaction in the presence of DTNB; Open circles (○) are data points obtained by quenching reaction mixtures are regular intervals, followed by DTNB treatment. All data points represent the average of two separate measurements, with the errors bars indicating the standard deviation. Linear regression analysis of the (●) data set gives a line with the equation $y = 0.6763x + 0.000138$. The y-axis labels on the left and right are associated with the data points to the left and right of the x-axis break respectively; the units are identical in both cases.

under the assay conditions used, the kinetics of the Smiles rearrangement do not adversely affect the measurement of MshB's deacetylation of **3b** by DTNB derivatization.

The finding that MshB's activity towards **3b** as a substrate correlates linearly over the concentration range used (0–5 mM) was not surprising considering that the K_M value determined for GlcNAc using the FSA assay is 38 ± 4 mM (k_{cat} 46 ± 2.2 min^{-1}).[21] However, the poor solubility of **3b** in aqueous solutions prevented us from using higher concentrations, and therefore the kinetic parameters could not be determined for this substrate. Nonetheless, the rate obtained for 5 mM GlcNAc-SDNP using the DTNB-based assay is ~7–12% of the k_{cat}(GlcNAc) obtained in the FSA-(46 ± 2.2 min^{-1})[21] and HPLC-based (29.4 ± 2.4 min^{-1})[27] assays respectively, suggesting that the kinetic parameters for **3b** do not differ significantly from those for GlcNAc.

Finally, the result demonstrates that GlcNAc-SDNP **3b** acts as a suitable alternative substrate for MshB, allowing its activity to be measured continuously using a DTNB-based assay at concentrations as low as 50 μM.

Conclusions

In this study we set out to develop a new continuous assay of MshB activity based on the use of chromogenic substrates. In the process, we uncovered an unexpected and previously unseen enzyme-initiated Smiles rearrangement of one of the substrates.

This discovery allowed for the first continuous and sensitive assay of MshB activity to be developed.

The study of the mechanistic detail of the Smiles rearrangement of deacetylated **3b** would be interesting considering not only the novelty of the enzyme-based initiation of the reaction, but would also help relate the rate of deacetylation to the kinetic and thermodynamic factors that control the formation and subsequent collapse of the associated Meisenheimer complex. Moreover, it is also unclear whether the Smiles rearrangement takes place in the MshB active site, where interaction between the unmasked thiol and the catalytic metal ion may result in inhibition, or only after the deacetylated product is released. However, it is quite likely that the rearrangement takes place upon collapse of the tetrahedral intermediate, and that adjacent acidic residues such as His144 plays a role in stabilizing the Meisenheimer complex intermediate. Conversely, the very rigid platform provided by the glucosamine skeleton, and the presence of stabilising electron-withdrawing nitro substituents in **3b**, would promote the rearrangement independent of enzyme involvement. A full understanding of the interplay between such considerations would be helpful in further establishing the utility of the assay.

In conclusion, the serendipitous discovery of GlcNAc-SDNP **3b** as an alternate MshB substrate with unique characteristics provides the opportunity for microplate-based inhibitor screening of this enzyme, or any other deacetylase reactivity that may potentiate the Smiles rearrangement by similarly invoking heteroatom nucleophiles. This finding may significantly advance our search of inhibitors of mycothiol biosynthesis as potential antituberculosis agents.

Materials and methods

General reagents and methods

Chemicals were purchased from Sigma-Aldrich. All reactions were performed at room temperature unless specified otherwise. Flash chromatography was performed using a 20 : 1 weight ratio of silica to crude reaction mixture. Thin layer chromatography (TLC) was performed on Merck Aluminium Silica gel 60 F_{254} plates. All compounds containing free amines were visualized on TLC plates by spraying the plates with ninhydrin solution (1.5% ninhydrin in *n*-butanol with 3% AcOH) followed by heating the plates until the colour developed. All chromogenic compounds were visualized on the TLC plate under UV light. HPLC analyses were performed on an Agilent 1100 system with an in-line DAD detector. LC-HR-ESI-MS analyses were performed using a Waters Aquity UPLC attached to a Waters Synapt G2 QTOF mass spectrometer. High resolution ESI-MS analyses were performed on a QTOF Ultima API quadrupole mass spectrometer. ^{1}H and ^{13}C NMR was performed on Varian Unity Inova 600 MHz NMR and Varian VXR 300 MHz NMR spectrometers. Enzyme assays (fluorometric and spectrophotometric analyses) were conducted using a Varioskan multimode reader (Thermo Scientific). An extinction coefficient (ε) of 13 600 dm^{-3} mol^{-1} cm^{-1} was used for the absorbance of 2-nitro-5-thiobenzoate (NTB, **8**) at 412 nm.

Computational methods

Prior to performing the docking calculations the MshB crystal structure (PDB ID: 1Q74) was protonated using the Karlsberg pK_a prediction tool.[30] The protein was hydrated for molecular dynamics (MD) simulations using a sphere of 30.0 Å in a manner similar to one reported previously.[31]

MD simulations were performed using the CHARMM32b[32] program with the CHARMM27 all atom force field for the protein[33] and CSFF for the carbohydrate and inositol.[34] In all MD simulations a water sphere of 30.0 Å containing 11 322 TIP3P[35] water molecules as implemented in CHARMM[36] were used. The system was centred about the glycosidic linkage of the ligand for the simulations. The water molecules that overlapped with any of the ligand heavy atoms were removed and a spherical boundary force was applied to the surface of the water sphere to maintain a consistent water density of 1.0 g cm^{-1}. A constant temperature of 298.15 K was maintained throughout the simulations using the Nosé–Hover thermostat.[37] A buffer region of 2 Å thickness and a dynamic region with 21 Å radius was used with Langevin dynamics in all simulations. All hydrogen bond lengths were kept fixed with the SHAKE algorithm and an integration step of 1 fs was used.

The crystal structure was subjected to 7 ns explicitly solvated molecular dynamics and then stripped of water molecules, after which several ligands were docked in the MD solution equilibrated MshB structure using Glide.[38] A cubic volume of side 9 Å, centred on the central zinc atom was selected. A search was conducted *via* a grid generation with no constraints in conjunction with a Van der Waals scaling factor of 1 and a partial charge cut-off of 0.25. Conformational searches on each ligand were performed using the *Extra Precision* (XP) algorithm, where a maximum of 2000 conjugate gradient steps, a distance dielectric cut-off of 2 Å and flexible docking were applied on 1200 poses for every ligand.

Of the conformations generated, those where the Coulomb and van der Waals interactions summed to values greater than 0 were rejected. To ensure that the ligands generated were conformationally distinct an RMS deviation of 0.5 Å was used. The 100 highest scoring geometries for each molecule were examined to identify structures where the carbonyl carbon is in close proximity to the zinc.

Synthesis of α-thioglycoside compounds

4-Nitrophenyl 2-acetamido-2-deoxy-1-thio-3,4,6-tri-*O*-acetyl-α-D-glucopyranose (5a). To a solution of compound **4**[26] (280 mg, 0.773 mmol) in 5 ml dichloromethane stirred under a N_2 atmosphere was added 1-fluoro-4-nitrobenzene (164 μl, 2.8 mmol) and triethylamine (130 μl, 1.15 mmol). The reaction was allowed to stir for 24 h, and then concentrated. The product was purified from the crude reaction mixture using flash chromatography (2% MeOH/CH_2Cl_2), resulting in 360 mg (96% yield) of pure **5a** as a yellow amorphous solid. δ_H (600 MHz, $CDCl_3$, Me_4Si): 1.974 (s, 3H), 2.026 (s, 3H), 2.061 (s, 3H), 2.081 (s, 3H), 4.070 (dd, 1H), 4.254 (dd, 1H), 4.373 (m, 1H), 4.590 (m, 1H), 5.169 (m, 2H), 5.902 (d, 1H), 6.013 (d, 1H), 7.560 (d, 2H), 8.152 (d, 2H); δ_C (150 MHz, CD_3COCD_3): 21.9, 23.9, 54.3,

64.0, 71.1, 71.5, 72.3, 87.6, 126.0, 132.0, 145.5, 171.8, 171.9 and 207.4. *m/z* (100% ESI-MS): 485 [M + H]$^+$, 507 [M + Na]$^+$.

2,4-Dinitrophenyl 2-acetamido-2-deoxy-1-thio-3,4,6-tri-*O*-acetyl-α-D-glucopyranose (5b). To a solution of compound **4**[26] (500 mg, 1.37 mmol) in 10 ml dichloromethane stirred under a N$_2$ atmosphere was added 1-fluoro-2,4-dinitrobenzene (173 μl, 1.37 mmol) and triethylamine (230 μl, 1.65 mmol). The mixture was allowed to stir under a N$_2$ atmosphere for 24 h. The reaction mixture was then concentrated and the resulting product was purified using flash chromatography (2% MeOH/CH$_2$Cl$_2$), resulting in 570 mg (79% yield) of pure **5b** as a yellow solid. δ_H (300 MHz, CDCl$_3$, Me$_4$Si): 1.935 (s, 3H), 1.991 (s, 3H), 2.034 (s, 3H), 2.066 (s, 3H), 4.043 (dd, 1H), 4.265 (m, 2H), 4.626 (m, 2H), 5.235 (m, 2H), 6.100 (d, 1H), 8.045 (d, 1H), 8.406 (dd, 1H), 9.026 (d, 1H); *m/z* (100% ESI-MS): 530 [M + H]$^+$.

Benzyl 2-acetamido-2-deoxy-1-thio-3,4,6-tri-*O*-acetyl-α-D-glucopyranose (5c). To a solution of compound **4**[26] (220 mg, 0.61 mmol) in 2 ml dichloromethane stirred under a N$_2$ atmosphere was added benzylbromide (87 μl, 0.732 mmol) and triethylamine (170 μl, 1.22 mmol). The reaction mixture was allowed to stir under a N$_2$ atmosphere for 24 h. Subsequently the reaction was concentrated and the resulting product was purified using flash chromatography (2% MeOH/CH$_2$Cl$_2$), resulting in 170 mg (62% yield) of pure **5c** as an off white oil. δ_H (400 MHz, CD$_3$OD, Me$_4$Si): 1.89 (s, 3H), 1.93 (s, 3H), 2.01 (s, 3H), 2.06 (s, 3H), 3.81 (d, 2H), 3.98 (d, 1H), 4.24 (dd, 1H), 4.38 (m, 3H), 4.97 (dd, 1H), 5.16 (dd, 1H), 5.29 (d, 1H) and 7.30 (m, 5H). δ_C (100 MHz, CD$_3$OD, Me$_4$Si): 20.4, 22.1, 35.0, 52.9, 63.1, 69.3, 70.6, 71.9, 83.8, 128.1, 129.4, 129.9, 138.9 and 171.2.

4-Nitrophenyl 2-acetamido-2-deoxy-1-thio-α-D-glucopyranose (3a). To a solution of **5a** (230 mg, 0.475 mmol) in 18 ml of H$_2$O (19%), MeOH (50%) and acetone (31%), was added 2.3 g of Amberlite IRA-400 (OH$^-$). The reaction mixture was allowed to stir for 1 h at ambient temperature. The volatile solvents were removed *in vacuo* and the residual aqueous product mixture was subjected to C$_{18}$ flash chromatography (50% MeCN/H$_2$O). Aqueous fractions containing the compound were collected and dried by lyophilization, resulting in 50 mg (29% yield) of pure **3a** as an amorphous yellow solid. δ_H (300 MHz, CD$_3$OD, Me$_4$Si): 1.99 (s, 3H), 3.44 (t, 1H), 3.74 (m, 3H), 3.97 (m, 1H), 4.15 (dd, 1H), 6.08 (d, 1H), 7.68 (d, 2H) and 8.15 (d, 2H). δ_C (75 MHz, CD$_3$OD, Me$_4$Si): 22.5, 56.1, 62.4, 72.3, 72.6, 75.7, 87.3, 124.9, 130.6, 146.3, 147.5 and 173.9. *m/z* (100% ESI-HRMS): 359.0929 ([M + H]$^+$ C$_{14}$H$_{19}$N$_2$O$_7$S$^+$ requires 359.0913).

2,4-Dinitrophenyl 2-acetamido-2-deoxy-1-thio-α-D-gluco-pyranose (3b). Prepared as for **3a** from **5b** (230 mg, 0.434 mmol), resulting in 60 mg (34% yield) of **3b** as an amorphous yellow solid. δ_H (300 MHz, (CD$_3$)$_2$SO, Me$_4$Si): 1.829 (s, 3H), 3.264 (m, 1H), 3.516 (q, 1H), 3.588 (m, 2H), 3.674 (m, 1H), 3.983 (m, 1H), 4.554 (t, 1H), 5.125 (d, 1H), 5.272 (d, 1H), 6.051 (d, 1H), 8.150 (d, 1H), 8.273 (d, 1H), 8.426 (dd, 1H), 8.818 (d, 1H). *m/z* (100% ESI-HRMS): 404.0781 ([M + H]$^+$ C$_{14}$H$_{18}$N$_3$O$_9$S$^+$ requires 404.0764).

Benzyl 2-acetamido-2-deoxy-1-thio-α-D-glucopyranose (3c). Prepared as for **3a** from **5c** (230 mg, 0.507 mmol), resulting in 76 mg (38% yield) of **3c**. m.p. 192–194 °C (dec). δ_H (300 MHz, CD$_3$OD, Me$_4$Si): 1.89 (s, 3H), 3.36 (dd, 1H), 3.60 (dd, 1H), 3.76 (m, 4H), 3.99 (m, 2H), 5.34 (d, 1H), 7.20 (t, 1H), 7.27 (t, 2H) and 7.33 (d, 2H). δ_C (75 MHz, CD$_3$OD, Me$_4$Si): 22.5, 35.0, 55.6, 62.6, 72.6, 74.5, 84.0, 128.0, 129.4, 130.1, 139.6, 173.5 and 173.5. *m/z* (100% ESI-HRMS): 328.1211 ([M + H]$^+$ C$_{15}$H$_{22}$NO$_5$S$^+$ requires 328.1219).

MshB preparation

The *mshB* (Rv1170) gene was amplified from *M. tuberculosis* H37Rv genomic DNA using as forward primer 5′-GGTGCCTCCATGGCTGAGACGCCGC-3′ and as reverse primer 5′-CCTGGTTGGCCTCGAGCGTGCCGGAC-3′. The primers respectively contained NcoI and XhoI restriction enzyme sites (underlined), while the reverse primer also removed the native stop codon. The resulting PCR product was treated with NcoI and XhoI and ligated to similarly treated pET28a(+) to yield the expression vector pET28a(+)-*mshB* that encodes recombinant MshB with a C-terminal 6×His-tag. The plasmid's sequence was confirmed by DNA sequencing.

For the expression of MshB the pET28a(+)-*mshB* plasmid was transformed (heat shock method) into *E. coli* BL21*(DE3) cells. LB medium (500 ml) was inoculated with a 5 ml starter culture of these cells grown in the same medium, followed by cell growth at 37 °C until the culture reached an OD$_{600}$ of 0.6. Expression was induced by the addition of IPTG to a final concentration of 0.10 mM, after which the culture was incubated overnight at 22 °C. Cells were harvested by centrifugation at 17 000 × *g* for 20 min at 10 °C. The resulting cell pellet was resuspended in binding buffer (20 mM Tris–HCl, 5 mM imidazole, 500 mM NaCl, pH 7.9), and the cells were disrupted using sonication with external cooling (ice bath). Cell debris were removed by centrifugation at 75 000 × *g* for 20 min at 10 °C to obtain the clarified cell extract used for purification.

The protein was purified using an automated purification program on an ÄKTA*prime* system (Amersham Bioscience) fitted with a 1 ml HiTrap Chelating HP column (GE Healthcare) pre-loaded with Zn^{2+}. The column-bound MshB was eluted with 100% elution buffer (20 mM Tris-HCl, 500 mM imidazole, 500 mM NaCl, pH 7.9) and desalted using a 5 ml HiTrap desalting column (GE Healthcare) with gel filtration buffer (25 mM Tris-HCl, 5 mM MgCl$_2$, 5% glycerol, pH 8) on the ÄKTA*prime* system. Protein purity was confirmed with SDS-PAGE analyses and protein concentration was determined with a Bradford assay. Pure MshB (in gel filtration buffer with 5% glycerol added) was aliquoted and stored at −80 °C until needed.

HPLC-based activity analysis

All samples used for the direct HPLC analysis of MshB activity contained one of the thioglycoside substrates (**3a**, **3b** or **3c**) at a final concentration of 0.1 mM, assay buffer (50 mM HEPES, 50 mM NaCl, <1% DMSO, pH 7.4) and MshB (16.7 μg; 2 μM) in a total volume of 250 μl. Reactions were initiated with the addition of MshB. Samples of the reaction were stopped at

5286 | *Org. Biomol. Chem.*, 2012, **10**, 5278–5288

This journal is © The Royal Society of Chemistry 2012

intervals of 5 min over a period of 20 min by heat inactivation, followed by removal of the denatured enzyme by centrifugation at 12 000 × g for 5 min to obtain the clarified samples used for HPLC analysis.

For the determination of the substrate concentrations in the samples, standard solutions of **3a–c** with a concentration range of 0–120 μM and a final volume of 250 μl each were given the same treatment as the enzyme reaction samples before these were also analysed by HPLC. From these results a standard curve which correlated peak area with concentration was obtained for each substrate.

Samples of 5 μl each were injected on to a Synergi 4μ Fusion-RP 250 × 2.00 mm column (Phenomenex) and eluted using aqueous acetonitrile as solvent. The amount of acetonitrile used differed for each substrate: for GlcNAc-SPNP (**3a**), 30% MeCN/H₂O; for GlcNAc-SDNP (**3b**), 25% MeCN/H₂O; and for GlcNAc-SBn (**3c**), 40% MeCN/H₂O. Separation was monitored at 320 nm for **3a** and **3b**, and at 254 nm for **3c**.

FSA- and DTNB-based activity analyses

Reaction mixtures (250 μl) containing the respective substrate (5 mM) in assay buffer (50 mM HEPES, 50 mM NaCl, 1 mM TCEP, 5–10% DMSO, pH 7.5) and MshB (8.1 μg; 1 μM) were incubated at 30 °C. Samples (30 μl) of the reaction mixture were added at 10 min intervals to 10 μl trichloroacetic acid (TCA) (1.22 M) to quench the reaction, followed by removal of the precipitated protein by centrifugation at 12 000 × g for 5 min. The supernatant (25 μl) was subsequently added to 75 μl borate buffer (1 M, pH 9).

For the fluorescamine (FSA)-based analysis, 49 μl of the resulting mixture was added to 30 μl of FSA (10 mM) contained in a 96-well microplate incubated at room temperature, after which the fluorescence was determined using an excitation wavelength of 395 nm, and an emission wavelength of 485 nm.

For the 5,5′-dithiobis-(2-nitrobenzoic acid) (DTNB)-based analysis, 49 μl of the resulting mixture was diluted to 100 μl, and then added to 30 μl DTNB (2.2 mM) contained in a 96-well microplate. After incubation at room temperature for 10 min, the absorbance at 412 nm was determined.

LC-HR-ESI-MS analyses

Reaction mixtures (100 μl) contained GlcNAc-SDNP (**3b**) (0.7 mM) in assay buffer (50 mM HEPES, 50 mM NaCl, ~5% DMSO, pH 7.5) (the enzyme was omitted from a negative control reaction). One set of reaction mixtures also contained 1 mM TCEP. Mixtures were equilibrated at 30 °C for 10 min before MshB (1 μM final concentration) was added, followed by incubation at 30 °C for 1 h. The reaction was quenched by adding two 45 μl aliquots from each mixture to two separate microfuge tubes containing 15 μl TCA (6.12 M) each. The precipitated protein was removed by centrifugation at 12 000 × g for 5 min, after which the supernatants from each tube (37.5 μl) were added to 112.5 μl borate buffer (1 M, pH 9) contained in two separate microfuge tubes. The tubes subsequently received either 45 μl acetonitrile or 45 μl DTNB (0.72 mM in acetonitrile) prior to LC-HR-ESI-MS analysis.

Reaction mixtures were analysed on a Waters Aquity UPLC system with an autosampler using a Synergi 4μ Fusion-RP 250 × 2.00 mm column (Phenomenex). The sample injection volume was 20 μl and the autosampler syringe was washed with solvent A (0.1% formic acid in water) before each injection. A gradient elution program with a flow-rate of 0.30 ml min⁻¹ was used for the analysis. The gradient was as follows: 0–6 min, linear increase to 50% solvent B (0.1% formic acid in acetonitrile); 6–8 min, isocratic 50% B; 8–10 min, linear increase to 95% solvent B. Detection was performed on a Waters Synapt G2 QTOF mass spectrometer. Analytes were detected in the positive and negative ion mode using a capillary voltage of 3000 V, cone voltages of 15 V and a source temperature of 150 °C. The mass spectrometer was calibrated with sodium formate and Leu-enkephalin as internal standard to acquire the lock mass for the HR-ESI-MS analysis. Data processing was done using MassLynx (Waters).

Continuous DTNB-based MshB assay

Reaction mixtures (125 μl) contained GlcNAc-SDNP (**3b**) (0–5 mM) in assay buffer (50 mM HEPES, 50 mM NaCl, ~10% DMSO, pH 7.5) with DTNB (0.75 mM) and MshB (10 μg; 2.5 μM) were incubated at 30 °C in a 96-well microplate, and the increase in absorbance at 412 nm was monitored over a period of 30 min. Reaction rates were determined by linear regression of the resulting progress curves obtained between 5–30 min. Discontinuous reaction monitoring was performed as before, using the same reaction mixture without DTNB and withdrawing 30 μl aliquots at set time intervals for processing and analysis as described above.

Acknowledgements

References

1 J. A. Imlay, *Annu. Rev. Microbiol.*, 2003, **57**, 395–418; J. A. Imlay, *Annu. Rev. Biochem.*, 2008, **77**, 755–776.
2 P. Zuber, *Annu. Rev. Microbiol.*, 2009, **63**, 575–597.
3 G. L. Newton, K. Arnold, M. S. Price, C. Sherrill, S. B. Delcardayre, Y. Aharonowitz, G. Cohen, J. Davies, R. C. Fahey and C. Davis, *J. Bacteriol.*, 1996, **178**, 1990–1995; R. C. Fahey, *Annu. Rev. Microbiol.*, 2001, **55**, 333–356; G. L. Newton, M. Rawat, C. J. J. La, V. K. Jothivasan, T. Budiarto, C. J. Hamilton, A. Claiborne, J. D. Helmann and R. C. Fahey, *Nat. Chem. Biol.*, 2009, **5**, 625–627; J. D. Helmann, *Antioxid. Redox Signaling*, 2011, **15**, 123–133.
4 V. K. Jothivasan and C. J. Hamilton, *Nat. Prod. Rep.*, 2008, **25**, 1091–1117.
5 G. L. Newton, N. Buchmeier and R. C. Fahey, *Microbiol. Mol. Biol. Rev.*, 2008, **72**, 471–494.
6 M. Rawat, C. Johnson, V. Cadiz and Y. Av-Gay, *Biochem. Biophys. Res. Commun.*, 2007, **363**, 71–76.

This journal is © The Royal Society of Chemistry 2012

Org. Biomol. Chem., 2012, **10**, 5278–5288 | 5287

7   C. Bornemann, M. A. Jardine, H. S. C. Spies and D. J. Steenkamp, *Biochem. J.*, 1997, **325**, 623–629.

8   G. L. Newton, P. Ta, K. P. Bzymek and R. C. Fahey, *J. Biol. Chem.*, 2006, **281**, 33910–33920.

9   C. J. Hamilton, R. M. J. Finlay, M. J. G. Stewart and A. Bonner, *Anal. Biochem.*, 2009, **388**, 91–96.

10 C. M. Holsclaw, W. B. Muse, III, K. S. Carroll and J. A. Leary, *Int. J. Mass Spectrom.*, 2011, **305**, 151–156; M. P. Patel and J. S. Blanchard, *Biochemistry*, 2001, **40**, 5119–5126; K. S. E. Ung and Y. Av-Gay, *FEBS Lett.*, 2006, **580**, 2712–2716.

11 M. Steffek, G. L. Newton, Y. Av-Gay and R. C. Fahey, *Biochemistry*, 2003, **42**, 12067–12076.

12 M. Rawat, S. Kovacevic, H. Billman-Jacobe and Y. Av-Gay, *Microbiology*, 2003, **149**, 1341–1349; X. Xu, C. Vilcheze, Y. Av-Gay, A. Gomez-Velasco and W. R. Jacobs, Jr., *Antimicrob. Agents Chemother.*, 2011, **55**, 3133–3139.

13 M. Hernick and C. A. Fierke, *Arch. Biochem. Biophys.*, 2005, **433**, 71–84.

14 X. Huang, E. Kocabas and M. Hernick, *J. Biol. Chem.*, 2011, **286**, 20275–20282.

15 A. A. McCarthy, N. A. Peterson, R. Knijff and E. N. Baker, *J. Mol. Biol.*, 2004, **335**, 1131–1141.

16 J. T. Maynes, C. Garen, M. M. Cherney, G. Newton, D. Arad, Y. Av-Gay, R. C. Fahey and M. N. G. James, *J. Biol. Chem.*, 2003, **278**, 47166–47170.

17 X. Huang and M. Hernick, *J. Biol. Chem.*, 2012, **287**, 10424–10434.

18 G. M. Nicholas, L. L. Eckman, P. Kovac, S. Otero-Quintero and C. A. Bewley, *Bioorg. Med. Chem.*, 2003, **11**, 2641–2647; M. A. Jardine, H. S. C. Spies, C. M. Nkambule, D. W. Gammon and D. J. Steenkamp, *Bioorg. Med. Chem.*, 2002, **10**, 875–881; K. Ajayi, V. V. Thakur, R. C. Lapo and S. Knapp, *Org. Lett.*, 2010, **12**, 2630–2633; S. Lee and J. P. N. Rosazza, *Org. Lett.*, 2004, **6**, 365–368.

19 S. Knapp, S. Gonzalez, D. S. Myers, L. L. Eckman and C. A. Bewley, *Org. Lett.*, 2002, **4**, 4337–4339.

20 G. L. Newton, Y. Av-Gay and R. C. Fahey, *J. Bacteriol.*, 2000, **182**, 6958–6963.

21 X. Huang and M. Hernick, *Anal. Biochem.*, 2011, **414**, 278–281.

22 D. W. Gammon, D. J. Steenkamp, V. Mavumengwana, M. J. Marakalala, T. T. Mudzunga, R. Hunter and M. Munyololo, *Bioorg. Med. Chem.*, 2010, **18**, 2501–2514.

23 G. M. Nicholas, L. L. Eckman, G. L. Newton, R. C. Fahey, S. Ray and C. A. Bewley, *Bioorg. Med. Chem.*, 2003, **11**, 601–608.

24 B. B. Metaferia, B. J. Fetterolf, S. Shazad-ul-Hussan, M. Moravec, J. A. Smith, S. Ray, M.-T. Gutierrez-Lugo and C. A. Bewley, *J. Med. Chem.*, 2007, **50**, 6326–6336.

25 S. Knapp, B. Amorelli, E. Darout, C. C. Ventocilla, L. M. Goldman, R. A. Huhn and E. C. Minnihan, *J. Carbohydr. Chem.*, 2005, **24**, 103–130; B. Paul and W. Korytnyk, *Carbohydr. Res.*, 1984, **126**, 27–43; Y. Ding, Y. Miura, J. R. Etchison, H. H. Freeze and O. Hindsgaul, *J. Carbohydr. Chem.*, 1999, **18**, 471–475.

26 S. Knapp and D. S. Myers, *J. Org. Chem.*, 2002, **67**, 2995–2999; S. Knapp and D. S. Myers, *J. Org. Chem.*, 2001, **66**, 3636–3638.

27 G. L. Newton, M. Ko, P. Ta, Y. Av-Gay and R. C. Fahey, *Protein Expression Purif.*, 2006, **47**, 542–550.

28 H. Kondo, F. Moriuchi and J. Sunamoto, *J. Org. Chem.*, 1981, **46**, 1333–1336.

29 W. E. Truce, E. M. Kreider and W. W. Brand, *Org. React.*, 2011, 99–215.

30 B. Rabenstein and E.-W. Knapp, *Biophys. J.*, 2001, **80**, 1141–1150; G. Kieseritzky and E.-W. Knapp, *Proteins: Struct., Funct., Bioinf.*, 2008, **71**, 1335–1348.

31 K. J. Naidoo, D. Denysyk and J. W. Brady, *Protein Eng., Des. Sel.*, 1997, **10**, 1249–1261; K. J. Naidoo and J. W. Brady, *THEOCHEM*, 1997, **395–396**, 469–475.

32 B. R. Brooks, R. E. Bruccoleri, B. D. Olafson, D. J. States, S. Swaminathan and M. Karplus, *J. Comput. Chem.*, 1983, **4**, 187–217; B. R. Brooks, C. L. Brooks, A. D. Mackerell, L. Nilsson, R. J. Petrella, B. Roux, Y. Won, G. Archontis, C. Bartels, S. Boresch, A. Caflisch, L. Caves, Q. Cui, A. R. Dinner, M. Feig, S. Fischer, J. Gao, M. Hodoscek, W. Im, K. Kuczera, T. Lazaridis, J. Ma, V. Ovchinnikov, E. Paci, R. W. Pastor, C. B. Post, J. Z. Pu, M. Schaefer, B. Tidor, R. M. Venable, H. L. Woodcock, X. Wu, W. Yang, D. M. York and M. Karplus, *J. Comput. Chem.*, 2009, **30**, 1545–1614.

33 A. D. MacKerell, D. Bashford, M. Bellott, R. L. Dunbrack, J. D. Evanseck, M. J. Field, S. Fischer, J. Gao, H. Guo, S. Ha, D. Joseph-McCarthy, L. Kuchnir, K. Kuczera, F. T. K. Lau, C. Mattos, S. Michnick, T. Ngo, D. T. Nguyen, B. Prodhom, W. E. Reiher, B. Roux, M. Schlenkrich, J. C. Smith, R. Stote, J. Straub, M. Watanabe, J. Wiórkiewicz-Kuczera, D. Yin and M. Karplus, *J. Phys. Chem. B*, 1998, **102**, 3586–3616.

34 M. Kuttel, J. W. Brady and K. J. Naidoo, *J. Comput. Chem.*, 2002, **23**, 1236–1243.

35 W. L. Jorgensen, J. Chandrasekhar, J. D. Madura, R. W. Impey and M. L. Klein, *J. Chem. Phys.*, 1983, **79**, 926–935.

36 P. J. Steinbach and B. R. Brooks, *Proc. Natl. Acad. Sci. U. S. A.*, 1993, **90**, 9135–9139.

37 S. Nosé, *Mol. Phys.*, 1984, **52**, 255–268; W. G. Hoover, *Phys. Rev. A: At., Mol., Opt. Phys.*, 1985, **31**, 1695–1697.

38 B. Hammouda, *J. Polym. Sci., Part B: Polym. Phys.*, 1992, **30**, 1387–1390.